

Oops They Did It Again! Carbon Nanotubes Hoax Scientists in Viability Assays

J. M. Wörle-Knirsch, K. Pulskamp, and H. F. Krug*

*Forschungszentrum Karlsruhe, Institute of Toxicology and Genetics,
Department of Molecular and Environmental Toxicology, P.O. Box 3640,
D-76021 Karlsruhe, Germany*

Received January 25, 2006; Revised Manuscript Received March 29, 2006

ABSTRACT

New materials of emerging technological importance are single-walled carbon nanotubes (SWCNTs). Because SWCNTs will be used in commercial products in huge amounts, their effects on human health and the environment have been addressed in several studies. Inhalation studies in vivo and submerge applications in vitro have been described with diverging results. Why some indicate a strong cytotoxicity and some do not is what we report on here. Data from A549 cells incubated with carbon nanotubes fake a strong cytotoxic effect within the MTT assay after 24 h that reaches roughly 50%, whereas the same treatment with SWCNTs, but detection with WST-1, reveals no cytotoxicity. LDH, FACS-assisted mitochondrial membrane potential determination, and Annexin-V/PI staining also reveal no cytotoxicity. SWCNTs appear to interact with some tetrazolium salts such as MTT but not with others (such as WST-1, INT, XTT). This interference does not seem to affect the enzymatic reaction but lies rather in the insoluble nature of MTT–formazan. Our findings strongly suggest verifying cytotoxicity data with at least two or more independent test systems for this new class of materials (nanomaterials). Moreover, we intensely recommend standardizing nanotoxicological assays with regard to the material used: there is a clear need for reference materials. MTT–formazan crystals formed in the MTT reaction are lumped with nanotubes and offer a potential mechanism to guide bioremediation and clearance for SWCNTs from “contaminated” tissue. SWCNTs are good supporting materials for tissue growth, as attachment of focal adhesions and connections to the cytoskeleton suggest.

Introduction. Nanoparticles and nanomaterials can be on the same scale as elements of living cells, including proteins, nucleic acids, lipids and cellular organelles. When considering nanoparticles it must be asked how man-made nanostructures can interact with or influence biological systems. On one hand, nanosystems are specifically engineered to interact with biological systems for particular medical or biological applications. On the other hand, the large-scale production of nanoparticles for either nonmedical applications or as the side products of combustion processes may affect a wide range of organisms throughout the environment. There have been an increasing number of investigations concerning the use of nanoscale structures since the 1970s; for example, liposomes for drug transport and comparable applications have been undertaken.^{1–5} In addition to liposomes, nanoparticles produced from other materials came into the focus of physicians for various disease treatments.^{6,7} The goal of these works has been to design inert auxiliary accompanying materials and to use body-friendly and

biodegradable excipients. However, dependent on their target organ and functionality, not all of these materials are degradable and some stay in the body for long periods of time. Thus, long-term side effects and foreign body reactions may be detectable and a good local and systemic tolerance during and after medication should be a condition *sine qua non*. Nanostructured materials come into contact with biological systems through their use in drug delivery systems or for gene transfer. They are also produced for food and cosmetic chemistry and many other technical applications.⁸ The increasing production, particularly of single-walled carbon nanotubes, will enhance the possible exposure at workplaces, packing stations, and during application of these products.⁹ In addition, waste treatment and containment at the end of a product's life cycle must be considered. Because of all of these reasons, it is of great interest to determine how these materials, when coming into contact with living organisms, are taken up, transported in or through cell layers,¹⁰ and possibly affect biological functions. In this report we focus on the toxicity of single-walled carbon nanotubes (SWCNTs) with their unique functions for electronics, engineering and biomedical applications, and as sensors. Among the new carbon modifications described

* Corresponding author. E-mail: krug@itg.fzk.de. Address: Forschungszentrum Karlsruhe, Department of Molecular and Environmental Toxicology, Institute of Toxicology and Genetics – ITG, P.O. Box 3640, D-76021 Karlsruhe, Germany. Phone: + 49 7247 82 3262. Fax: + 49 7247 82 3557.

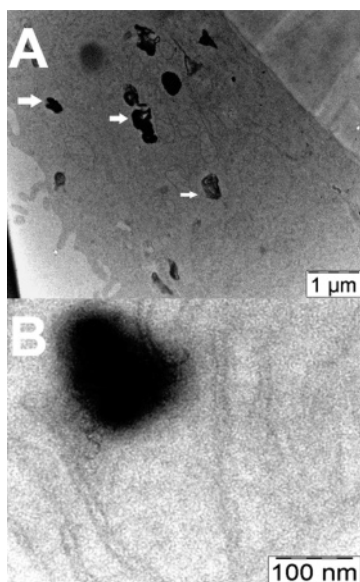


Figure 1. TEM preparations of SWCNTs inside human epithelial lung cells 24 h after incubation. Nanotubes can be found as bundles of thousands inside epithelial cells (arrowheads). SWCNTs are mostly encapsulated in endosomes or, as found here in B, can also be located inside mitochondria.

recently in many publications,^{8,11–17} SWCNTs have a very special and prominent position. Their physical features and mechanical strength are so interesting that people found them suitable for building space elevators and other robust constructions.¹⁸ Again, for other reasons they can be used as computer components in microprocessors or conductors. Upon electrification, they can emit light and therefore have the potential to drive displays and novel light-emitting diodes. In medical therapy they are used as drug carriers or to transport DNA from one organism to the other.^{19,20} All of this is fascinating and interesting, even if technologists lack behind in realizing these dreams. Problems in separating the different CNT types dominate the workload. Hence, everyday somewhere in the world someone discovers a better method for producing CNTs, a better way of handling them, and an even better preparation of functionalizing them. Nevertheless, it was found that CNTs can have a toxic potential to human health^{21–24} as was demonstrated in mice and rats. Most of the toxicological studies were carried out *in vitro* by very well-standardized protocols. We demonstrate here that the uncritical publication of toxicity data for these new nanomaterials may present false positive results, which in fact can turn against this new technology.

Therefore, investigations on and for a safe use of nanotechnology in science and industry are desirable.

Results. When human A549 lung epithelial-like cells as well as other cell types were exposed to SWCNTs over a time period of more than 12 h, single-walled carbon nanotubes can be found within the cells. The transmission electron micrographs in Figure 1 show SWCNT bundles inside cells (Figure 1A) and rarely inside mitochondria as well (Figure 1B). Moreover, the nanotube bundles are surrounded by a membrane in most of our preparations. Single nanotubes could not be detected because their size

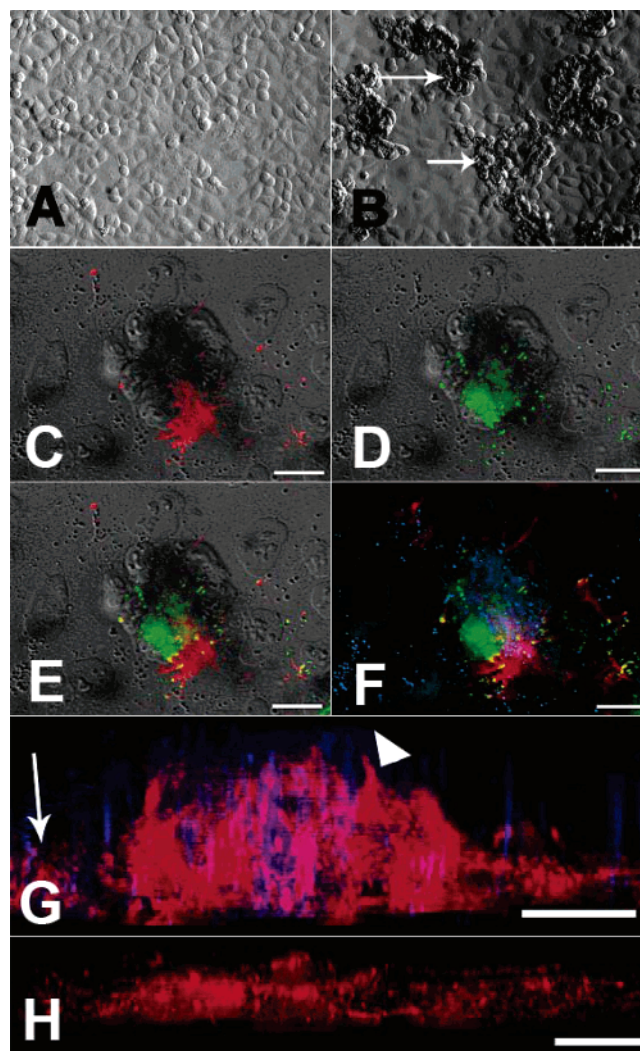


Figure 2. Light micrographs of human epithelial A549 cells grown to confluence 24 h after exposure with SWCNTs. Human A549 cells untreated (A) or treated with metal-reduced (B) SWCNTs for 24 h. Arrows point to aggregates formed within the confluent cell layer. Cells grow over bundles of SWCNTs rapidly enclosing this xenobiotic (magnification 200x). Accumulation of SWCNTs (black and blue) with focal adhesion kinase (FAK; green) and the cytoskeletal actin filaments (red). Immunohistochemistry with SWCNTs 24 h after incubation (C–F). Subconfluent grown cells were challenged with SWCNTs; these adhere to the cells and form agglomerates around the site of attachment. This is an active process as can be seen by complexation of FAK and actin filaments near the site of intrusion. Virtual cross section from 3D processed digital image (G) showing cells extending from the plane into open space attached to SWCNTs (blue). Arrows point to actin in the plain, whereas cells tightly attached to the nanotube bundle are successfully growing out of the surface cell layer (arrowheads); in the control (H) this cannot be observed (scale bar 15 μ m).

(with a diameter of about 1.4 nm) is on the scale of cellular components, and therefore they disappear in the background.

Light micrographs taken 24 h after exposure with catalyst-reduced SWCNTs in a concentration of 50 μ g/mL show strong accumulation of cells around a possible incorporation site of SWCNTs in the cell culture (Figure 2 B). These pictures give a representative impression of how many of these cell agglomerates are formed within a monolayer cell culture. The absolute number of these agglomerations is not

increased over time (data not shown) and does not differ between A549 and ECV cells. The untreated control (Figure 2A) displays a confluent layer of cells where no agglomerations can be found. Figure 2C–F shows a strong accumulation of focal adhesion kinase (D) (FAK; green) and the cytoskeletal actin filaments (C) (red) in the neighborhood of SWCNTs (black and blue) in human epithelial-like cells in an DIC overlay image (E). Immunohistochemistry to visualize the attachment of SWCNTs to cell elements reveals an association with focal adhesions and the cellular actin cytoskeleton. When cells were grown in subconfluent culture and challenged with SWCNTs, the tubes adhere to the cells and the cells start to form agglomerates around the site of attachment. This seems to be an active process because strong condensation of actin filaments and FAK could be observed in the overlay image of SWCNTs, actin, and FAK (Figure 2F). The nanotube bundles are actively anchored to the cells and kept at this location; the cells start to detach from the culture dish and grow out of the plain. This tendency to form agglomerates may explain the formation of granuloma in animals.^{21,23} A virtual cross section of such an agglomerate is displayed in Figure 2G. This image shows the actin filaments of all cells surrounding a bundle of nanotubes. It can be seen that actin staining is ubiquitously present in all cells, but it remains on the bottom surface (arrows) of the control cell monolayer (H). The behavior of the cells changes totally after addition of SWCNT bundles, and the cells begin to move out of the monolayer to attach to the SWCNTs, forming colony-like structures (G; arrowheads). This demonstrates that SWCNTs can serve as excellent substrates for mammalian cells to grow on. For a three-dimensional image and movie of a SWCNT bundle located inside such a cell agglomerate, please see the Supporting Information (Figure S2).

Measuring the viability of cells after incubation with chemicals is a routinely made method in toxicological laboratories to gain and assess toxicity information. The MTT salt is reduced by mitochondrial dehydrogenases to the water-insoluble MTT–formazan, then extracted and photometrically quantified at 550 nm. Therefore, the untreated cells are used as positive control (100% viable) and all values from the experiment are correlated with this set of data. When applying the MTT assay to cells incubated with SWCNTs, an obvious loss in viability can be measured (Figure 3). The reduction in cell viability reaches almost 60% after 24 h. This reduction is confirmed here in several experiments in parallel and with at least four repeats. The viability loss cannot be increased with longer incubation times for SWCNTs or within a range of concentrations used (10 up to 200 $\mu\text{g/mL}$, data not shown). Reduction of viability is consistent over time and is hardly affected by any parameter or cell type used.

Another standard assay that is used widely for analysis of acute cytotoxicity is the WST assay. We used this assay to confirm our results from the MTT assay. Again, a tetrazolium salt is reduced by cellular mitochondrial dehydrogenases at the same structural position when compared to MTT. The resulting product is, in contrast to MTT–formazan from the

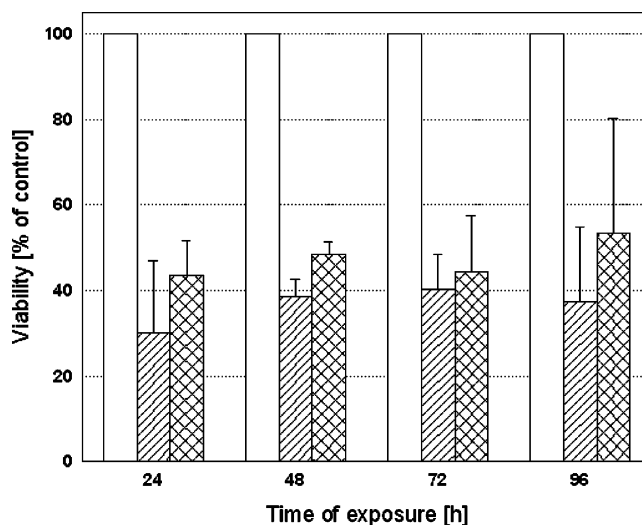


Figure 3. MTT assay after incubation with carbon nanotubes in A549 cells in a concentration of 50 $\mu\text{g/mL}$ for indicated times. Reduction of MTT to formazan suggests here a reduction in viability upon SWCNT treatment to values below 50% compared to control (open bars). Viability from cells treated with either SWCNTs without (hatched) or with catalyst metals (crosshatched) did not differ significantly and did not increase or decrease over the time period observed ($n \geq 4$).

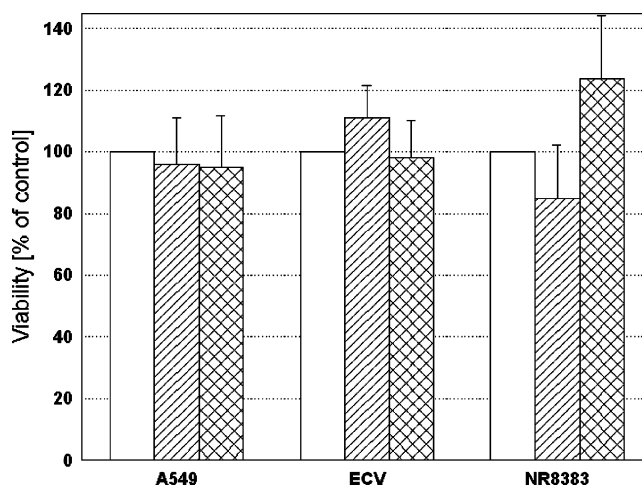


Figure 4. WST-1 assay on A549, ECV, and NR8383 cells incubated for 24 h with carbon nanotubes [50 $\mu\text{g/mL}$]. The reduction of WST-1 is unaffected by SWCNTs, and cells remain viable to approximately 100% as compared to the control (open bars). No significant changes in viability between the two SWCNT samples as prepared (hatched) and purified (crosshatched) can be observed after 24 h ($n \geq 4$) in either cell line exposed.

MTT assay, water-soluble and can be photometrically quantified at 450 nm. When applying SWCNTs to human cells in culture, no reduction in viability can be detected with the WST assay (Figure 4) in epithelial (A549), endothelial (ECV), or rat macrophages (NR8383).

Living cells keep the integrity of their plasma membrane up because it is crucial for sustaining ion homeostasis over the surrounding media. In mitochondria the intact membrane is also necessary to gain energy from a proton gradient. This lactate dehydrogenase assay (LDH) is a marker for membrane integrity in cells and therefore for cell viability. The enzyme LDH is freely located in the cytoplasm and upon membrane

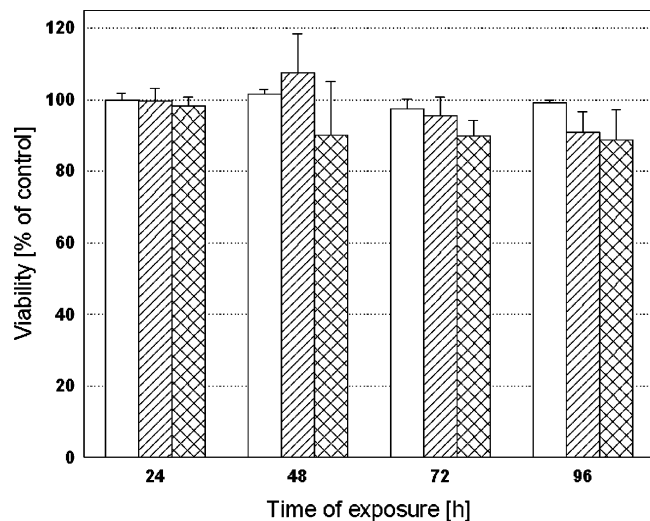


Figure 5. Cytotoxicity detection with lactate dehydrogenase assay (LDH) in A549 cells treated with 50 $\mu\text{g/mL}$ carbon nanotubes for the indicated times. The tetrazolium salt INT used in the LDH reaction here is not affected by addition of SWCNTs to cells. Control (open bars) and SWCNTs with (hatched) and without metal catalyst residues (crosshatched) are all around 100% viability, not differing significantly from the control, indicating no acute toxicity for this material ($n \geq 4$).

damage release into the surrounding media should occur. This assay detects the presence of LDH in the medium indirectly because the tetrazolium salt INT is reduced in a LDH-dependent reaction with this assay. Incubation of several cell lines (A549, ECV304) with SWCNTs for 24 h and longer and at different concentrations was tested. No reduction in viability can be observed here (Figure 5), and changes in concentration or incubation time again have no significant influence on cell viability. The produced INT–formazan here is a water soluble one as for the WST assay.

Most viability assays, such as MTT and WST, function by a reduction of a detectable product by specific enzymes, thereby determining physiological active cells, classifying these as vital. TMRE is a quantitative marker for the activity of mitochondria, which requires no metabolic action of the cell. The higher the TMRE fluorescence, the higher the concentration of dye inside the mitochondria. This fluorescence determines the actual mitochondrial membrane potential (MMP). Treatment of cells with SWCNTs does not lead to a loss in cell viability or loss of functionality of mitochondria (Figure 6). The MMP remains unchanged upon treatment as can be measured by a high TMRE fluorescence that is at or above 100% of control mitochondria equally treated, but kept SWCNT-free. These new carbon modifications do not have an influence on this parameter.

Flow cytometry using Annexin-V and propidium iodide additionally present no indication for a loss in viability caused by SWCNT incubation by neither necrosis nor apoptosis (data not shown).

The electron micrographs (Figure 7) show SWCNTs after treatment in various conditions as transmission electron micrographs. In Figure 7A, SWCNTs that were incubated for 24 h in growth media alone can be seen. These nanotubes exhibit the well-described appearance.^{18,32,33} The average

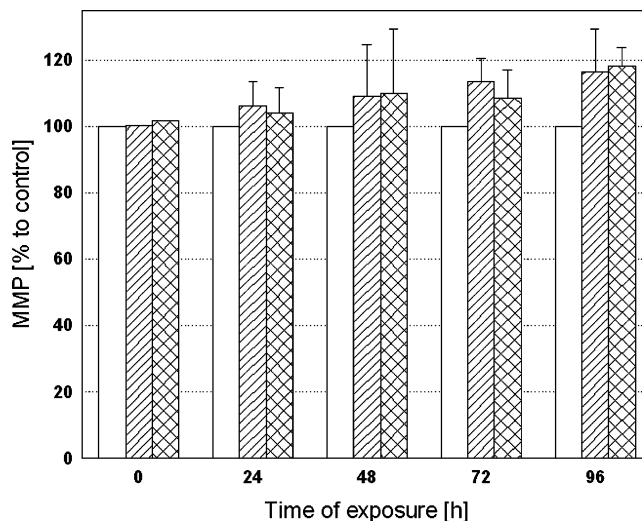


Figure 6. Mitochondrial membrane potential (MMP) as measured by TMRE fluorescence in A549 cells with carbon nanotubes incubated for indicated times. TMRE dye in the untreated control at the indicated time points serves as a reference parameter and is set to 100% (open bars). The displayed mitochondrial membrane potential is of cells with SWCNTs either without (hatched) or with (crosshatched) metal catalyst. Membrane potential remains stable in A549 cells treated with SWCNTs [50 $\mu\text{g/mL}$] for several time points and offers no indication of impairment of mitochondrial enzyme reactions. Cells appear to be fully viable ($n \geq 4$).

diameter of a SWCNT is between 1.2 and 1.4 nm with variable length; this has been described for many preparations in several publications. In Figure 7B SWCNTs are depicted that have been incubated with cells for 24 h and 2 h with WST-1 and then extracted. Again, the structure of the SWCNT is not changed, no attachments are visible, and no modifications can be seen. In Figure 7C SWCNTs are depicted that have been incubated for 24 h with cells and for 2 h with MTT.

This MTT is reduced to MTT–formazan by the mitochondria, here in the presence of SWCNTs in the living cell. In contrast to the other samples in Figure 7C, the SWCNTs appear in this electron micrograph with MTT–formazan crystals that are covering the nanotubes, clumping everything together. This mixture cannot be solved with SDS, 2-propanol/HCl, or acetone (data not shown). Even heat treatment (60 $^{\circ}\text{C}$, 10 min) is not successful in removing the crystals from the SWCNTs and bringing MTT–formazan into solution. A reduction in MTT–formazan content in the MTT assay may be due to a loss of crystals to the SWCNTs. When WST-1 preparation from SWCNTs is observed in TEM, no structural changes can be seen for either extraction method (data not shown). It is therefore a MTT-specific phenomenon.

Discussion. Since their discovery in the 1980s, carbon nanotubes are told to have a great potential for both science and industry. Elevators into space have been postulated and bridges that can be carried by men and other fantastic things have been imagined to be possible with carbon nanotubes. Their stability and lightweight features fueled dreams. Their unique properties in terms of electric conductance, light-emitting features, and metallic character made them so

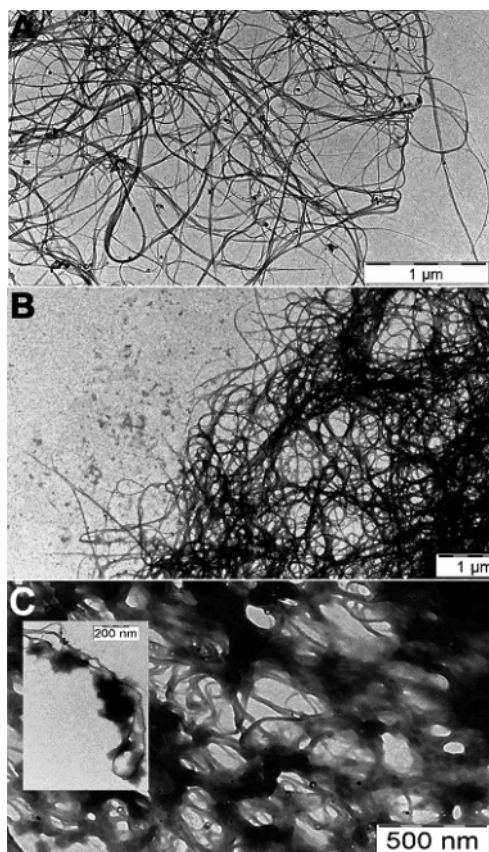


Figure 7. TEM preparations of SWCNTs after incubation with human A549 cells for 24 h in complete media and extraction with 2-propanol/HCl. Crude preparations of SWCNTs after incubation in media (without MTT) and cells for 24 h and after 2-propanol/HCl extraction can be seen in A. This picture shows the regular and well-known appearance of SWCNTs without any structural particularities. In B WST-1 was added 2 h prior to extraction; full recovery of WST-1 formazan leaves no crystals behind. However, in C a structural change in the SWCNTs can be seen with strong distinctions all over the SWCNT meshwork, which might be formazan crystals that cannot be resolved.

special. More recently, nanotechnologists have learned to handle these fibers and start to understand why they are so special.

Nevertheless, a loud public outcry happened when in 2004 Eva Oberdörster published that bucky balls can lead to lipid peroxidation in the brain of juvenile fish.^{34,35} Because bucky balls or fullerenes are structurally and chemically related to CNTs, people started thinking about possible negative side effects for this material too. Thus, some works have been published on the toxicity of this and other carbonaceous materials.^{22,34,36–46} Surprisingly, those who planned to use SWCNTs for biomedical purposes^{43,44,47} or gene/DNA transfer applications^{40,46} did not detect a cytotoxic effect, whereas the more environmental or toxicological oriented groups did.^{38–42}

For the assessment of acute cytotoxicity, several methods have been developed that are applicable and well-described in the literature. MTT, WST, XTT, and LDH are just a few among those to be named here. For this new class of materials (nanomaterials), the viability assay of choice has to be double-checked because interferences and disturbances

are likely to happen, as described here. SWCNTs do interact with MTT–formazan crystals, formed after reduction of MTT and not with water-soluble tetrazolium salts such as WST-1, XTT, or INT. SWCNTs bind MTT–formazan crystals and stabilize their chemical structure, and, as a consequence, these crystals cannot be solubilized in 2-propanol/HCl, SDS, or acetone. The MTT–formazan crystals can be found within or attached to carbon nanotubes (Figure 7C).

This has been demonstrated in a great effort of using multiple viability assays with identical data for several cell lines and nanotube concentrations. As one can see from the TEM pictures (Figure 7) and the viability assays (Figure 3), the reduction from tetrazolium salts to formazan is working. The heterocycle with the four nitrogen atoms is accessible for mitochondrial dehydrogenases, and this reaction is not blocked by SWCNTs, as demonstrated by the positive results within the LDH and WST-1 assay and confirmed by others.⁴⁸ The dehydrogenases attack the same position in the tetrazolium salts and open the tetrazolium ring. No inhibition of the mitochondrial enzymes could be observed because WST-1 catalysis is unaffected (Figure 4), which is dependent on the same enzymes as MTT-reduction. The chemical substitutions in the tetrazolium salts (MTT – two methyl groups, WST-1 and INT – nitro group) or the thiazolyl cycle in the MTT molecule are the only possible interaction partners for the nanotubes. It appears that the insolubility of the MTT–formazan is crucial for attachment to the nanotubes and disturbance of the test. No clumping of MTT crystals can be found for the other tetrazolium salt-generated formazans (Figure 7) as demonstrated by TEM images and positive reduction of WST-1 and LDH (Figure 4, 5). Hence, our results suggest that there is no acute toxicity for carbon nanotubes. So far, it has never been described for a nanomaterial to interfere directly with a cytotoxicity assay agent. Our findings strongly suggest verifying cytotoxicity data with at least two or more independent test systems for this new class of materials (nanomaterials). It has been described that nanotubes exhibit various effects on biomolecules, such as stimulation as well as inhibition of the polymerase chain reaction.⁴⁹ Moreover, studies with living organisms indicate adverse effects for CNTs in mice and rats,^{21,23,24} and a comparable cell agglomeration in vitro has been shown here (Figure 2B). The lung granuloma as well as the accumulation of cells in culture in close proximity of larger CNT bundles suggest an attractive role of CNT surfaces without acute toxicity.

Therefore, further experiments with regard to biological and chemical aspects of this phenomenon have to be carried out. The following has to be clarified: if the reduction of MTT and the formation of MTT–formazan–SWCNT clusters offer a mechanism suitable for biofunctionalization of CNTs in a very effective manner, and how mitochondrial reductases gain access to the tubes. This might give good insight into bioremediation tools and about nanotube clearance after medical treatment as suggested by some.

Acute toxicity has been described in several studies published recently.^{22,39,41,48,50} Among these, a broad variety

of cell types and lines have been used. In vivo studies compared to in vitro experiments show mostly different results but cannot be compared. The knowledge, so far available, consists of data on the basis of a nonstandardized CNT material; thus, all of these studies including our presented data have to be considered as isolated and not directly comparable experiments. One very important point regarding toxicity is the variation of impurities of the different CNT preparations. Most used fractions contain high amounts of metals, such as iron and nickel.^{9,21} The toxicity of high concentrations of these metals is well-known. Another very important contamination is amorphous carbon, which exhibits comparable biological effects as carbon black or relevant ambient air particles.^{51–54} We compared CNT samples of different purity and tried to separate CNTs from metals as well as from amorphous carbon. These very pure CNTs lose in our hands their capacity to induce acute toxicity or oxidative stress (data not shown). However, in vivo experiments demonstrated pathological observations that resemble the behavior of the cells in vitro in our experiments. The formation of granuloma shown by Warheit²³ and Lam²¹ in vivo indicate a cellular attraction by CNTs and we observed this in vitro in a similar manner. The oxidative stress as well as the induction of inflammatory processes seem to correlate directly with remaining amorphous carbon, Ni, Fe, and other heavy metals. To address the poor dispersion properties of CNTs in water, one must establish a uniform protocol for sample preparation. In particular, description of sonification procedures and solvents used for separation of tubes from bundles must be comprehensible. Hence, there is a clear need for a standardized CNT reference material to be used by all toxicologists in order to make toxicological data comparable between the different studies as was done for DEP (diesel exhaust particles).

Materials and Methods. Cell Culturing. The human alveolar epithelial cell line A549 (ATCC, CCL-185)^{25,26} was obtained from American Type Culture Collection (Rockville, MD), and endothelial cells derived from umbilical cord were obtained as a cell line (ECV304) from the European Collection of Cell Cultures. The rat alveolar macrophage cell line (NR8383) was obtained from American Type Culture Collection (Rockville, MD). NR8383 cells were grown in F-12K medium (Kaighn's Modification, Gibco) supplemented with 15% heat-inactivated fetal calf serum (FCS). Human A549 cells were grown in Dulbecco's modified Eagle's medium (DMEM, Invitrogen, Karlsruhe), and ECV304 cells were grown in M199 media, both supplemented with 10% heat inactivated FCS, 2 mM L-glutamine, all supplied with 100 µg/mL penicillin and 100 U/mL streptomycin. The cells were grown in a humidified incubator at 37 °C (95% room air, 5% CO₂).

Single-Walled Carbon Nanotube (SWCNT) Preparation. Carbon nanotube synthesis was performed by F. Hennrich (Institute for Nanotechnology, Karlsruhe, Germany) at the University of Karlsruhe in Prof. Kappes lab with the laser vaporization method described earlier.^{27,28} These single-walled carbon nanotubes have been used for biological experiments with a metal catalyst content (mainly Co and

Table 1. Elemental Composition of SWCNT Preparations (in weight %)

material	C	O	N	H	Co	Ni
as prepared:	78.3	7.1	1.1	2.6	4.3	4.3
acid treated:	65.7	25.3	1.5	2.7	1.3	1.2

Ni) of approximately 8 wt % or catalyst reduced (2.5%). Therefore, acid treatment to elute catalyst metals was performed as described previously.²⁷ All nanotube preparations were stored in a 1% SDS solution. Before use in the experiment, SWCNTs were acetone precipitated (21000 xg) and resuspended in bidistilled water, sedimented again by centrifugation, and finally taken up in growth media and diluted to final concentrations. Prior to use, samples were sonified (6 × 30 s, 70 W) and mixed vigorously to break up nanotube bundles and sediments. To keep the sample preparations free from other disturbing chemical additives such as DMSO or SDS (which facilitate CNT dispersion), we accepted a certain degree of CNT aggregation within our sample fluid. This was tolerable because we were interested in an observation of CNT toxicity as they may occupationally occur. Elemental composition was determined following air exposure. Carbon, oxygen, nitrogen, and hydrogen compositions were determined by IR spectroscopically analyzing combustion gases generated upon 1050 °C pyrolysis in pure oxygen. Weight percentages are accurate to 1, 3, 5, and 5% of the numbers given. Cobalt and nickel compositions were determined by atomic emission spectroscopy with standard dissolution methods. Metal compositions are accurate to within 3%. Note that the target rod contained small amounts of hydrogen and oxygen already, presumably deriving from the production process. This appears to be essentially transferred to the nanotube soot, as is the overall metal content. The soot is somewhat richer in oxygen than the target rod, likely because of the metal oxidation and gas adsorption in transfer.²⁷

Viability Tests. MTT Assay. Cells were grown in 96 well chambers overnight. For each set, 25 000 cells were seeded into every well of a 96-well plate (NUNC, Wiesbaden, Germany) in triplicate. Cells were treated with the described particle suspensions in a concentration of 50 µg/mL in complete culture medium for 24–96 h. Cytotoxicity was determined by measuring the reduction of the yellowish water-soluble MTT (3-(4,5-Dimethyl-2-thiazolyl)-2,5-diphenyl-2H-tetrazolium bromide, SIGMA) to water-insoluble MTT-formazan, after 2-propanol/HCl extraction at 550 nm. The results are given as relative values to the negative control in percent, whereas untreated (negative) control is set to be 100% viable.

WST-1 Assay. The tetrazolium salt 2-(4-iodophenyl)-3-(4-nitrophenyl)-5-(2,4-disulfophenyl)-2H-tetrazolium (SIGMA), better known as WST-1, was used to detect a loss in viability here. The 25 000 cells were incubated for the indicated times with SWCNTs in an identical experimental system as was used for the MTT assay. The reduced tetrazolium salt here is water-soluble; therefore, no 2-propanol/HCl extraction is necessary. Photometric quantification was performed at 450

nm in a microplate reader. Calculation was identical to that of the MTT test.

LDH Assay. Leaking membranes of damaged or dead cells release the cytoplasmic enzyme lactate dehydrogenase (LDH) into the surrounding media. This enzyme can be detected by measuring its catalytic activity and indirectly the conversion of 2-(4-Iodophenyl)-3-(4-nitrophenyl)-5-phenyl-2H-tetrazolium chloride (INT) to another water-soluble formazan dye. This test was performed with the Roche LDH detection kit (Roche Applied Science, Cytotoxicity Detection Kit) according to the manufacturer's instructions for an assay with 25 000 cells and variable SWCNT concentrations for several time points.

Mitochondrial Membrane Potential Determination. Tetramethylrhodamine ethyl ester (TMRE) measurement of the mitochondrial membrane potential (MMP) was carried out as described previously.^{29,30} Briefly, cells were stained with TMRE (500 nM; Molecular Probes, Leiden, The Netherlands) for 30 min at 37 °C and treated with SWCNTs for 24–96 h. As a positive control, 20 μ M FCCP (carbonyl cyanide 4-(trifluoromethoxy)phenylhydrazone, SIGMA, Germany) was added to the control sample to induce maximal loss in MMP by uncoupling oxidative phosphorylation and eliminating the mitochondrial proton gradient. Cells were subjected to flow cytometry, and the decrease in fluorescence intensity was analyzed using an excitation wavelength of 488 nm and emission wavelength of 520 nm.

TEM and Light Microscopy. SWCNTs were prepared either before or after incubation with cells, cells and MTT, MTT only, or SWCNTs alone in media for the indicated times. Particles were prepared as for use in the experiment and spotted on 75-mesh Formvar-coated copper grids and observed with a Zeiss 109T transmission electron microscope (Oberkochen, Germany) without contrast enhancement. Light micrographs (A–B) were taken with a Nikon (Coolpix 5000) digital still camera at a Nikon (Eclipse TS150) inverted stereo microscope at 200-fold magnification. Differential interference contrast (DIC) pictures (C–F) were made with a Zeiss Axiovert S100 inverted microscope (630x). For antibody staining, cells were fixated in 4% paraformaldehyde solution for 1 h in two chamber chamberslides (Nunc, Wiesbaden) on ice and made permeable with 0.1% Triton X 100 in 1% BSA in PBS for 1 h at room temperature. Primary antibody raised against focal adhesion kinase (FAK; BD Transduction Laboratories) was diluted 1:200 in 1% BSA, washed three times, and detected with a CY2 coupled secondary antibody 1:200 raised against anti-mouse IgG (Dianova) in 1% BSA. Actin cytoskeleton staining was done with phalloidin-rhodamine (Molecular Probes) diluted 1:30 in Phem-buffer³¹ for 2 h at 37 °C. Image analysis was done on an OpenLab imaging system (Improvision, U.K.). Generation of a 3D image was produced with deconvoluted images captured by Z-step procedure using 200-nm steps and the 3D module from OpenLab. For better visualizing, the co-localization of FAK, actin, and SWCNTs are displayed in blue as false color within the fluorescence images.

Acknowledgment. This work was supported by grants from the Forschungszentrum Karlsruhe and DFG-CFN E1.3

(Center for Functional Nanostructures). We thank M. Kappes and F. Hennrich (University of Karlsruhe and INT) for support and supply with SWCNTs.

Supporting Information Available: Three-dimensional movie of a SWCNT bundle located inside such a cell agglomerate (Figures S1 and 2) as a QuickTime movie produced with the Improvision OpenLab system. This material is available free of charge via the Internet at <http://pubs.acs.org>.

References

- (1) Agrawal, A. K.; Singhal, A.; Gupta, C. M. *Biochem. Biophys. Res. Commun.* **1987**, *148*, 357–361.
- (2) Clark, A. P. *Cancer Pract.* **1998**, *6*, 251–253.
- (3) Gregoriadis, G. *FEBS Lett.* **1973**, *36*, 292–296.
- (4) Gregoriadis, G.; Wills, E. J.; Swain, C. P.; Tavill, A. S. *Lancet* **1974**, *1*, 1313–1316.
- (5) Speiser, P. P. *Methods Find. Exp. Clin. Pharmacol.* **1991**, *13*, 337–342.
- (6) Allen, T. M.; Cullis, P. R. *Science* **2004**, *303*, 1818–1822.
- (7) Chen, Y.; Xue, Z.; Zheng, D.; Xia, K.; Zhao, Y.; Liu, T.; Long, Z.; Xia, J. *Curr. Gene Ther.* **2003**, *3*, 273–279.
- (8) Krug, H. F.; Kern, K.; Wörle-Knirsch, J. M.; Diabate, S. Toxicity of Nanomaterials – New Carbon Conformations and Metal Oxides. In *Impact of Nanomaterials on the Environment*; Kumar, C. S. S. R., Ed.; 2006, in press.
- (9) Maynard, A. D.; Baron, P. A.; Foley, M.; Shvedova, A. A.; Kisin, E. R.; Castranova, V. *J. Toxicol. Environ. Health, Part A* **2004**, *67*, 87–107.
- (10) Geys, J.; Coenegrachts, L.; Vercammen, J.; Engelborghs, Y.; Nemmar, A.; Nemery, B.; Hoet, P. H. *Toxicol. Lett.* **2006**, *160*, 218–226.
- (11) Borm, P. J.; Kreyling, W. *J. Nanosci. Nanotechnol.* **2004**, *4*, 521–531.
- (12) Da Ros, T.; Guldi, D. M.; Morales, A. F.; Leigh, D. A.; Prato, M.; Turco, R. *Org. Lett.* **2003**, *5*, 689–691.
- (13) Da Ros, T.; Spalluto, G.; Prato, M.; Saison-Behmoaras, T.; Boutorine, A.; Cacciari, B. *Curr. Med. Chem.* **2005**, *12*, 71–88.
- (14) Jianrong, C.; Yuqing, M.; Nongyue, H.; Xiaohua, W.; Sijiao, L. *Biotechnol. Adv.* **2004**, *22*, 505–518.
- (15) Tagmatarchis, N.; Shinohara, H. *Mini. Rev. Med. Chem.* **2001**, *1*, 339–348.
- (16) Tagmatarchis, N.; Georgakilas, V.; Prato, M.; Shinohara, H. *Chem. Commun. (Cambridge, U.K.)* **2002**, (18), 2010–2011.
- (17) Terrones, M.; Terrones, H. *Philos. Trans. R. Soc. London, Ser. A* **2003**, *361*, 2789–2806.
- (18) Yakobson, B. I.; Smalley, R. E. *Am. Sci.* **1997**, *85*, 324–337.
- (19) Kam, N. W.; Liu, Z.; Dai, H. *Angew. Chem. Int. Ed.* **2006**, *45*, 577–581.
- (20) Kam, N. W.; Liu, Z.; Dai, H. *J. Am. Chem. Soc.* **2005**, *127*, 12492–12493.
- (21) Lam, C. W.; James, J. T.; McCluskey, R.; Hunter, R. L. *Toxicol. Sci.* **2004**, *77*, 126–134.
- (22) Manna, S. K.; Sarkar, S.; Barr, J.; Wise, K.; Barrera, E. V.; Jejelowo, O.; Rice-Ficht, A. C.; Ramesh, G. T. *Nano. Lett.* **2005**, *5*, 1676–1684.
- (23) Warheit, D. B.; Laurence, B. R.; Reed, K. L.; Roach, D. H.; Reynolds, G. A.; Webb, T. R. *Toxicol. Sci.* **2004**, *77*, 117–125.
- (24) Shvedova, A. A.; Kisin, E. R.; Mercer, R.; Murray, A. R.; Johnson, V. J.; Potapovich, A. I.; Tyurina, Y. Y.; Gorelik, O.; Arepalli, S.; Schwegler-Berry, D.; Hubbs, A. F.; Antonini, J.; Evans, D. E.; Ku, B. K.; Ramsey, D.; Maynard, A.; Kagan, V. E.; Castranova, V.; Baron, P. *Am. J. Physiol.: Lung Cell Mol. Physiol.* **2005**, *66*, 1909–1926.
- (25) Giard, D. J.; Aaronson, S. A.; Todaro, G. J.; Arnstein, P.; Kersey, J. H.; Dosik, H.; Parks, W. P. *J. Natl. Cancer Inst.* **1973**, *51*, 1417–1423.
- (26) Lieber, M.; Smith, B.; Szakal, A.; Nelson-Rees, W.; Todaro, G. *Int. J. Cancer* **1976**, *17*, 62–70.
- (27) Hennrich, F.; Wellmann, R.; Malik, S.; Lebedkin, S.; Kappes, M. *Phys. Chem. Chem. Phys.* **2003**, *5*, 178–183.
- (28) Lebedkin, S.; Schweiss, P.; Renker, B.; Malik, S.; Hennrich, F.; Neumaier, M.; Stoermer, C.; Kappes, M. M. *Carbon* **2002**, *40*, 417–423.

- (29) Oberle, C.; Massing, U.; Krug, H. F. *Biol. Chem.* **2005**, *386*, 237–245.
- (30) Kamp, D. W.; Dunne, M.; Dykewicz, M. S.; Sbalchiero, J. S.; Weitzman, S. A.; Dunn, M. M. *J. Leukocyte Biol.* **1993**, *54*, 73–80.
- (31) Schliwa, M.; van Blerkom, J. J. *Cell Biol.* **1981**, *90*, 222–235.
- (32) Xu, Y. Q.; Peng, H.; Hauge, R. H.; Smalley, R. E. *Nano. Lett.* **2005**, *5*, 163–168.
- (33) Ericson, L. M.; Fan, H.; Peng, H.; Davis, V. A.; Zhou, W.; Sulpizio, J.; Wang, Y.; Booker, R.; Vavro, J.; Guthy, C.; Parra-Vasquez, A. N.; Kim, M. J.; Ramesh, S.; Saini, R. K.; Kittrell, C.; Lavin, G.; Schmidt, H.; Adams, W. W.; Billups, W. E.; Pasquali, M.; Hwang, W. F.; Hauge, R. H.; Fischer, J. E.; Smalley, R. E. *Science* **2004**, *305*, 1447–1450.
- (34) Oberdorster, E. *Environ. Health Perspect.* **2004**, *112*, 1058–1062.
- (35) Service, R. F. *Science* **2004**, *304*, 1732–1734.
- (36) Barlow, P. G.; Donaldson, K.; MacCallum, J.; Clouter, A.; Stone, V. *Toxicol. Lett.* **2005**, *155*, 397–401.
- (37) Pantarotto, D.; Briand, J. P.; Prato, M.; Bianco, A. *Chem. Commun. (Cambridge, U.K.)* **2004**, (1), 16–17.
- (38) Cui, D.; Tian, F.; Ozkan, C. S.; Wang, M.; Gao, H. *Toxicol. Lett.* **2005**, *155*, 73–85.
- (39) Jia, G.; Wang, H.; Yan, L.; Wang, X.; Pei, R.; Yan, T.; Zhao, Y.; Guo, X. *Environ. Sci. Technol.* **2005**, *39*, 1378–1383.
- (40) Lu, G.; Maragakis, P.; Kaxiras, E. *Nano. Lett.* **2005**, *5*, 897–900.
- (41) Monteiro-Riviere, N. A.; Nemanich, R. J.; Inman, A. O.; Wang, Y. Y.; Riviere, J. E. *Toxicol. Lett.* **2005**, *155*, 377–384.
- (42) Murr, L. E.; Esquivel, E. V.; Bang, J. J. *J. Mater. Sci.: Mater. Med.* **2004**, *15*, 237–247.
- (43) Pantarotto, D.; Singh, R.; McCarthy, D.; Erhardt, M.; Briand, J. P.; Prato, M.; Kostarelos, K.; Bianco, A. *Angew. Chem. Int. Ed.* **2004**, *43*, 5242–5246.
- (44) Shi Kam, N. W.; Jessop, T. C.; Wender, P. A.; Dai, H. *J. Am. Chem. Soc.* **2004**, *126*, 6850–6851.
- (45) Zheng, M.; Jagota, A.; Strano, M. S.; Santos, A. P.; Barone, P.; Chou, S. G.; Diner, B. A.; Dresselhaus, M. S.; McLean, R. S.; Onoa, G. B.; Samsonidze, G. G.; Semke, E. D.; Usrey, M.; Walls, D. J. *Science* **2003**, *302*, 1545–1548.
- (46) Zheng, M.; Jagota, A.; Semke, E. D.; Diner, B. A.; McLean, R. S.; Lustig, S. R.; Richardson, R. E.; Tassi, N. G. *Nat. Mater.* **2003**, *2*, 338–342.
- (47) Lovat, V.; Pantarotto, D.; Lagostena, L.; Cacciari, B.; Grandolfo, M.; Righi, M.; Spalluto, G.; Prato, M.; Ballerini, L. *Nano. Lett.* **2005**, *5*, 1107–1110.
- (48) Muller, J.; Huaux, F.; Moreau, N.; Misson, P.; Heilier, J. F.; Delos, M.; Arras, M.; Fonseca, A.; Nagy, J. B.; Lison, D. *Toxicol. Appl. Pharmacol.* **2005**, *207*, 221–231.
- (49) Cui, D.; Tian, F.; Kong, Y.; Titushikin, I.; Gao, H. *Nanotechnology* **2004**, *15*, 154–157.
- (50) Shvedova, A. A.; Castranova, V.; Kisin, E. R.; Schwegler-Berry, D.; Murray, A. R.; Gandelsman, V. Z.; Maynard, A.; Baron, P. J. *Toxicol. Environ. Health A* **2003**, *66*, 1909–1926.
- (51) Frampton, M. W.; Utell, M. J.; Zareba, W.; Oberdörster, G.; Cox, C.; Huang, L. S.; Morrow, P. E.; Lee, F. E.; Chalupa, D.; Frasier, L. M.; Speers, D. M.; Stewart, J. *Res. Rep. Health Eff. Inst.* **2004**, 1–47.
- (52) Gilmour, P. S.; Ziesenis, A.; Morrison, E. R.; Vickers, M. A.; Drost, E. M.; Ford, I.; Karg, E.; Mossa, C.; Schroepel, A.; Ferron, G. A.; Heyder, J.; Greaves, M.; MacNee, W.; Donaldson, K. *Toxicol. Appl. Pharmacol.* **2004**, *195*, 35–44.
- (53) Kim, Y. M.; Reed, W.; Lenz, A. G.; Jaspers, I.; Silbajoris, R.; Nick, H. S.; Samet, J. M. *Am. J. Physiol.: Lung Cell Mol. Physiol.* **2005**, *288*, L432–L441.
- (54) Lundborg, M.; Johard, U.; Lastbom, L.; Gerde, P.; Camner, P. *Environ. Res.* **2001**, *86*, 244–253.

NL060177C